Hall-Petch Relationship: Use in Characterizing Properties of Aluminum and Aluminum Alloys*

Ronald W. Armstrong
Department of Mechanical Engineering
University of Maryland
College Park, MD 21842

ABSTRACT

The mechanical properties of aluminum are shown to be of special importance beginning from the early 20th century production of the material in single crystal and polycrystalline form. Experimental and theoretical researches of the time were concerned with particular influence of polycrystalline microstructure and the presence of crystal (grain) boundaries on both the material strength properties and on relation of those same properties to those for the full range of metal and alloy structures. Now it is well-established that a relatively low value of the microstructural stress intensity, k_ε, obtains for aluminum in the generalized Hall-Petch relation for the stress - strain, σ_ε - ε, dependence on average grain diameter, ℓ, with intercept (friction) stress, $\sigma_{0\varepsilon}$, as

$$\sigma_\varepsilon = \sigma_{0\varepsilon} + k_\varepsilon \ell^{-1/2}.$$

With hindsight, taking $\sigma_\varepsilon = \sigma_{0\varepsilon}$ provided first connection between single crystal and polycrystalline strength measurements in the pioneering Taylor theory of plasticity proposed for aluminum and other face-centered cubic metals. Later conventional and ultrafine grain size measurements are shown to verify the fuller H-P dependence. The present account builds onto the early history. A description is given of temperature, strain rate, and alloy-dependent mechanical property measurements. An understanding of the total measurements is described in terms of a dislocation pile-up model description for the relation. Emphasis is given to k_ε for pure aluminum and related metals being determined by cross-slip being forced at grain boundaries. Particular attention is given to two characteristics of the metal mechanical behavior: {1} very high rate loading deformations leading to shock and *shock-less* isentropic compression experiments; and, {2} important grain size influences on nanopolycrystalline material behaviors. Additional results are presented on H-P aspects of the material strain ageing, shear banding, ductile fracturing and fatigue behaviors.

Introduction

An early assessment of newly-determined mechanical property measurements made on the 20th century face-centered cubic (fcc) metal, aluminum, took place at an important Faraday Society Meeting in 1927. Taylor, Polanyi and Gough, among other leading researchers, presented very different views on whether the presence of grain boundaries in aluminum should directly affect the relationship of single crystal and polycrystalline strength properties. Taylor argued for an absence of any direct grain boundary effect (1)

while Polanyi provided particular evidence that there must be an important influence (2). Gough, famous for research on fatigue, reported on torsional straining observations made of mutual grain interferences in testing a relatively large tri-crystal specimen. He concluded that the effect of the grain boundaries was mainly one of 'interference' due to the effect of the different crystal orientations (3). Taylor expressed the opinion that slip within an individual crystal was the same whether it was isolated or bounded by other crystals within a polycrystalline microstructure. The consideration led to a dislocation mechanics description of a parabolic σ_ε - ε curve for aluminum and related face-centered cubic metal single crystal deformation curves (4); and later, led to the notion that the constraint within mutually deforming (crystal) grains should require five independent deformation systems to operate within the individual grains so as to alleviate an arbitrary difference in the crystal-based strains tied to each grain orientation (5). As will be discussed, the analysis resulted in a Taylor orientation factor, m_T, to relate the single crystal resolved shear stress, τ_R, and the unidirectional tensile or compression value of flow stress, σ_ε; that is, $\sigma_\varepsilon = m_T\tau_R$. A value of $m_T = 3.08$ was calculated by Taylor. Only quite some years later did Kocks add to the model consideration by pointing to the Taylor requirement needing a comparative single crystal deformation curve undergoing *multi-slip* on the five requisite slip systems so that τ_R would be replaced by τ_M (6).

Polanyi's objection was expressed as "The interruption [of slip] at the grain boundary constrains the deformation, bringing about a thorough crumpling in the [grain] interior. It is to be expected that this constraint at the boundaries will be most strongly apparent in their immediate neighborhood. This is seen in the extension of a specimen consisting of two [aluminum] crystals, a ridge always forming at the boundary (Fig. 11)." And elsewhere in discussion at the meeting, Polanyi made the point that "the boundaries of crystals had a distinctly increased resistance against deformation, even if the crystals were of cubic structure. …". There is modern connection with Polanyi's argument given in a description of 'orange peel' effect associated with the surface roughness induced in large grain aluminum materials subjected to substantial plastic deformation (7). A compression test result was shown for a 7075-T6 aluminum alloy specimen subjected to large strain after which surface 'wrinkling' and macro-cracking started from micro-cracks initiated in the grain boundary 'valleys' of the wrinkles, particularly with greater concentration at the equatorial circumference of the bulged specimen. Such 'valleys' for the remaining-in-place grain boundaries provide the counterpart of Polanyi's 'ridges' on a tensile specimen.

A later update on consideration of the relationship between single crystal and polycrystalline metal plastic deformation was given by Chalmers in 1950 in another important conference on crystal plasticity (8). Taylor's description of five needed slip systems within the individual (crystal) grains was discussed in comparison with the need for taking into account more directly an influence of the material grain boundary properties/effects. The case for higher temperature weakening associated with the presence of grain boundaries was raised. In subsequent years, a number of deformation experiments were designed for application to aluminum bi-crystals 'grown' with grain boundaries either parallel (9) or perpendicular (10, 11) to the tensile axis. There is additional relation in the bi-crystal experiments of Pond and Harrison (11) to Polanyi's concern for a grain boundary resistance to displacement. Slip band rotations on either side of a grain boundary orthogonal to the tensile axis were shown to cause a sideways displacement of the essentially rigid boundary. Such rotations produced smaller specimen displacements on the crystal side where shorter slip band lengths impinged on the boundary. An important local observation was that the crystal boundary region exhibited smaller plastic strains in each case (10, 11). A modern aluminum bi-crystal reference involving more complex deformations that were forced to occur within a channel-die

geometry has been reported by Zaefferer, Kuo, Zhao, Winning and Raabe (12). Chalmers and Aust presented an important review of model grain boundary structures (13).

Substructure, Grain Boundaries and Subgrains

Very early recognition of the importance of a polycrystalline microstructure to determining strength properties has been tracked historically to the 18th century (14). Description of a model tetrakaidecahedron for an ideal polygonal grain shape exhibiting minimum surface area per unit volume is attributed in the 19th century to Lord Kelvin, as reviewed by Smith (15). Such shape consideration may be compared in the top level view of Fig. 1 to an average grain shape reported last century by Rhines, Craig and DeHoff for temperature-assisted grain growth in aluminum (16). The grain size is normally specified on a linear intercept basis that has advantage of specifying the grain surface area per unit volume independent of any shape consideration. Focus on the structure of grain boundaries and dislocation substructure within the grains, particularly for aluminum materials, has been a continuing modern research activity.

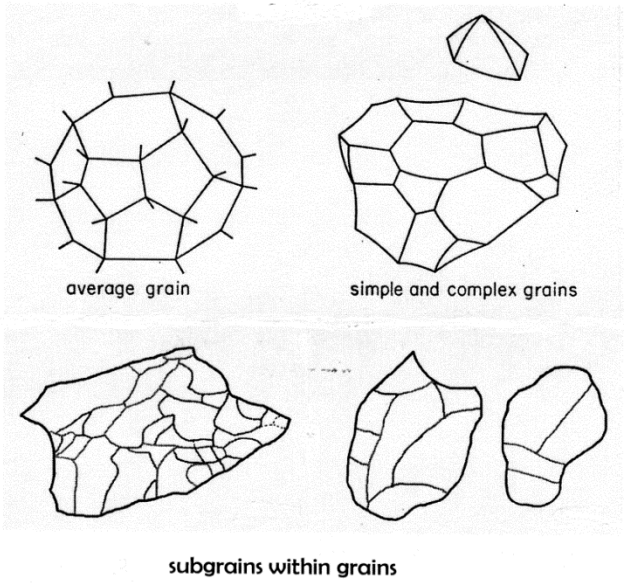

Figure 1. Grain and subgrain structures in aluminum

Hirsch had described pioneering measurements obtained with a micro-focus x-ray beam technique applied to determination of the dislocation densities in polycrystalline cold-worked aluminum (17). In the article Section on physical interpretation of the results, Hirsch began with the consideration that "During plastic flow the stresses around each grain will be non-uniform owing to the constraints imposed by the neighboring grains." The formation of subgrain boundaries by polygonization of like-sign dislocations was proposed to occur either during cold work or immediately thereafter. The work was followed up by breakthrough observations of individual dislocations in aluminum (18) by transmission electron microscopy (TEM). Dislocation arrangements in subgrain boundaries and motion of individual dislocations were observed in heavily cold-worked aluminum foils, including observation of dislocation cross-slip. An early TEM report on the structure of high angle grain boundaries in aluminum bi-crystals

was reported by Levy who also traced a bit of the early history in which grain boundaries were described as disordered regions (19). Le, Godfrey, Hansen, Liu, Winthur and Huang have reported more recently this century on the development of dislocation substructures generated within individual grains for a sintered aluminum polycrystalline material and subsequently deformed in compression by 20% (20).

In Fig. 1, the lower level images show the traces of subgrain boundary patterns within individual aluminum grains as described in detail *via* TEM by Le et al., including measurement of the subgrain boundary misorientation angles that, on the left side, were mostly in the range of 0-5° and on the right side were of 0-10°. Both measurements of subgrain misorientations are able to be fully accounted for in terms of crystal dislocations. The experimental observations relate to the consideration that dislocations provide both the vehicle by which plastic deformation is achieved and, when mutually intersected or piling up against subgrain boundary structures or 'tangles', provide significant resistance to continued deformation (21). Hong, Huang and Winthur have reported on such considerations for TEM measurements made of subgrain boundary networks produced in rolled aluminum material (22).

Other x-ray diffraction measurements have been reported for the effect of a resident dislocation substructure on the strength of aluminum materials, following on from Taylor originally pointing to the same type of x-ray asterism being observed in strained single crystal and polycrystalline material (1). Ball reported an inverse square root of subgrain size dependence of the flow stress of aluminum in which the subgrain size was specified *via* micro-focus x-ray diffraction measurements (23). Weissmann produced pioneering x-ray topographic images of individual aluminum grain deformations in a design of a modified Debye-Scherrer type x-ray system (24). Hultgren reported on the additive effect of grain and polygonized subgrain boundaries increasing the strength properties of aluminum materials (25). Additional hardening associated with an increasing mis-orientation of the subgrain boundaries was also determined. In a related model description of the strengthening properties associated with refractory metals, Armstrong, Bechtold and Begley had proposed the schematic description shown in Fig. 2 for the additive strengthening mechanisms (26). In the figure, the dislocations are seen as right-side up or inverted T's distributed with or without impurity/solute-associated black circles, also with a left-side solute-associated subgrain boundary and right-side grain boundary region with distributed solute segregation. The subgrain obstacle to slip penetration is weaker than that presented by a grain boundary.

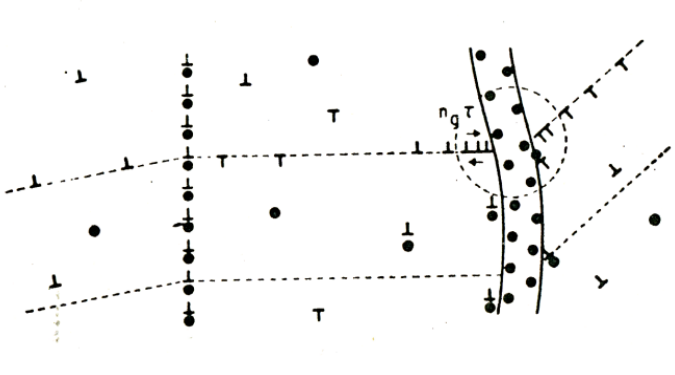

Figure 2. Schematic description of dislocation slip in a polycrystalline metal (26).

Hall-Petch measurements for aluminum

The eponymous Hall-Petch (H-P) relation reported for an inverse square root of grain diameter dependence of the yield and cleavage stresses of body-centered cubic (bcc) mild steel material (27, 28) provided what seems at first an unlikely alternative relationship to describe the much weaker grain size dependence of strength properties latterly measured for aluminum materials (29). Such later association was expressed in a generalized form of the grain size dependence extended beyond steel and related bcc metals to fcc and hexagonal close-packed (hcp) metals in the form:

$$\sigma_\varepsilon = m_T[\tau_{0\varepsilon} + k_{s\varepsilon}\ell^{-1/2}] \qquad [1]$$

In Eq. [1], m_T is the earlier-mentioned Taylor orientation factor, $\tau_{0\varepsilon}$ is the friction shear stress on dislocations in an average pile-up obstructed by a grain boundary requiring generation of a critical value of shear stress intensity, $k_{s\varepsilon}$, for overcoming the boundary resistance. In (29), a weak H-P dependence for aluminum was compared with a much stronger dependence observed for an aluminum-magnesium alloy, as will be discussed in connection with a large value of $k_{s\varepsilon}$ occurring for yield point behavior.

Comparison of Specimen Size and H-P Grain Size Dependencies

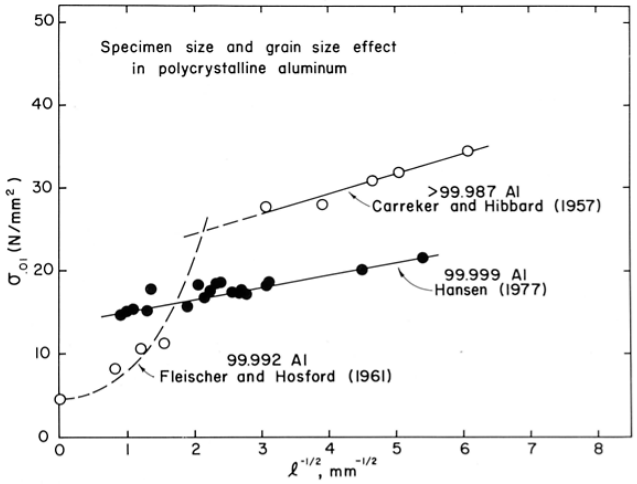

Figure 3. Single crystal, multi-crystal and true polycrystalline H-P dependencies for relatively pure aluminum materials (30-33).

A compilation of single crystal, multi-crystal and fully polycrystalline H-P yield stress or initial proof stress dependencies measured at ambient temperatures is shown for several relatively pure aluminum materials in Fig. 3 (30-33). The open-circle measurements, beginning from a single crystal tensile stress measurement on the ordinate axis with $\sigma_{.01} = 2\tau_{.01}$, are joined by the dashed curve indicating an increase in flow stress for an increasing number of grains in the specimen cross-section (32). The so-called specimen size effect is dependent on an increasing constraint between the grains occurring as the number of grains in the specimen cross-section builds up and leading to an H-P dependence for fully polycrystalline behavior (34). Thus, the inequality was established for an initial proof stress that

$$2\tau_R \leq \sigma_\varepsilon \leq m_T[\tau_M + k_{S\varepsilon}\ell^{-1/2}] \qquad [2]$$

The two H-P lines shown in Fig. 3 attest to the sensitivity of both $\sigma_{0\varepsilon}$ and k_ε to the presence of solute content in aluminum that has a relatively large solid solubility of elements compared to other metal systems. The lower filled-circle H-P measurements were obtained for fully polycrystalline flow beginning from the largest grain size points for which larger dimension specimens had been employed to insure a sufficient number of grains in the specimen cross-section, thus giving $m_T k_{S\varepsilon} = k_\varepsilon = 1.5$ MPa.mm$^{1/2}$ (33). The top-most open-circle points apply for other less pure material measurements obtained as part of a broader investigation of temperature and strain rate effects that are to be discussed (34). A value of $k_\varepsilon = 2.5$ MPa.mm$^{1/2}$ is obtained for these data. An early compilation of both $\sigma_{0\varepsilon}$ and k_ε values has been given for aluminum and for other fcc, bcc and hexagonal close-packed metals and alloys (35). More recent reports on the importance of specimen size effects in differentiating between single crystal and polycrystalline behavior have been reported: for pure aluminum by K.-H. Kim, H.-K. Kim and Oh (36); for 1100 aluminum by Kwon, Huh and Kim (37); and for nickel by Keller and Hug (38).

A later compilation of H-P measurements for the initial proof or yield stresses of a variety of 98.65 % or purer aluminum materials and covering a very large range in grain sizes was assembled by Wyrzykowski and Grabski as shown in Fig. 4 (39). An evaluation of the H-P slope values (microstructural stress intensities) were found to be in the range $0.3 \leq k_\varepsilon \leq 2.1$ MPa.mm$^{1/2}$ with average value of $k_\varepsilon = 1.3$ MPa.mm$^{1/2}$. The k_ε values compare with the two values of 1.5 and 2.5 MPa.mm$^{1/2}$ obtained from Fig. 1. A substantial range in values of $\sigma_{0\varepsilon}$ are seen directly in Fig. 4. Wyrzykowski and Grabski pointed to the importance of texture in accounting for the range in $\sigma_{0\varepsilon}$ values and to the mis-orientation character of the grain boundary structures in determining k_ε, thus relating to the observations of Hultgren (25) whose H-P dependence is marked by the number 9 in Fig. 4. The smallest 'grain size' results, marked 18-21 in the figure inset, are for ℓ taken as the subgrain size including number 19 for the referenced measurements of Ball (23). Armstrong had given an earlier comparison of H-P k_ε values based on both grain and subgrain sizes (40).

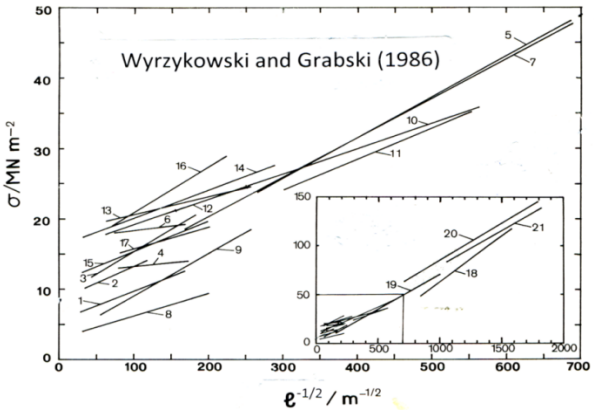

Figure 4. A compilation of H-P dependencies reported for relatively pure aluminum materials (39).

Strain, Temperature and Strain Rate Dependencies

The pioneering measurements made by Carreker and Hibbard (31) were reported without assessment in terms of the H-P parameters, $\sigma_{0\varepsilon}$ and k_ε, but nevertheless show on examination decreasing values of both parameters with increase in temperature, more so in $\sigma_{0\varepsilon}$. A weak strain rate dependence of the flow stress was measured by Carreker and Hibbard. Fujita and Tabata later reported measurements made of H-P yield and flow stress dependences at various ε values and at 77, 200, 293, 373, 473 K (41). At 293 K, the yield stress $k_y = 1.8$ MPa.mm$^{1/2}$ and was found to anomalously decrease with decrease in temperature. In addition, the post-yield stress H-P dependencies beginning at $\varepsilon \approx 0.03$ separated into two linear H-P relations. In a region of larger grain size, $1.3 \leq \ell^{-1/2} \leq 3.5$ mm$^{-1/2}$, relatively lower $\sigma_{0\varepsilon}$ and higher k_ε values were measured as compared with a same value of k_ε reported both for the yield stress and flow stress at smaller grain sizes up to $\ell^{-1/2} \leq 5.5$ mm$^{-1/2}$. Very likely, as will be seen, the reduced strain hardening that is reflected in the larger grain size flow stresses should be attributed to an influence of texture. Such result would be consistent with the general observation of k_ε being relatively larger when a well-defined yield point is observed but then to be followed by a relatively constant k_ε value for the flow stress dependence.

Hall-Petch dependencies have been measured also for the complete ambient temperature stress-strain behaviors of pure aluminum by Hansen (33, 42). Figure 5 shows the progressive H-P flow stress dependencies at a number of increasing tensile true strain values. The H-P dependence shown at $\varepsilon = 0.01$ is the same result shown in Fig. 3. Hanson importantly compared the $\sigma_{0\varepsilon}$ dependence on ε with the Taylor prediction of a parabolic σ_ε - ε dependence and with a single crystal $m_T\tau_M$ – ε measurement for a crystal with [111] tensile axis orientation to represent Kocks' multi-slip orientation (6). A satisfactory near-parabolic strain dependence was found but, somewhat surprisingly, better match was found with a lower Sachs orientation factor, $m_S = 2.24$, previously determined for activation, on average, of the so-called Schmid orientation factor for operation of a single fcc slip system over the full range of crystal orientations. The comparison could be interpreted as well to indicate that the average polycrystal grain does not experience strain hardening to the same extent as occurs for a [111] tensile axis single crystal. Also, Hansen made a comparison of the aluminum H-P dependence with a stronger one measured for copper (43), as also will be compared here in later discussion.

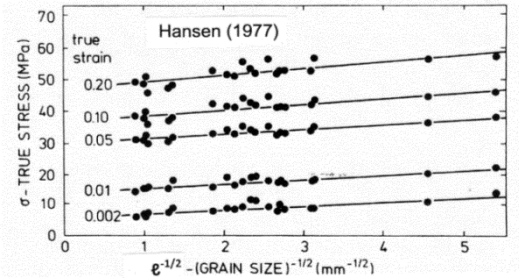

Figure 5. An H-P dependence for the stress-strain behavior of 99.99% aluminum (33).

Al-Haidary, Petch and de los Rios had obtained very comparable tensile results to those of Hansen at ambient temperature for both a super-pure 99.98% and commercial 99.2% material and reported additional measurements both at higher temperatures of 200 and 400°C (44) and at a lower temperature of 77 K (45). Except for a very low H-P dependence established for a proportional limit stress of $\sigma_0 \approx 3$ MPa and $k_0 \approx 0.7$ MPa.mm$^{1/2}$, the $\sigma_{.02}$ and higher flow stresses again gave a same $k_\varepsilon \approx 2$ to 2.5 MPa.mm$^{1/2}$

increasing with plastic strain to $\varepsilon = 0.20$ for the purer material. Comparison was made also with measurements made of a stronger H-P dependence for an aluminum-2.25% magnesium alloy, following on from the same comparison made between the Carreker and Hibbard aluminum measurements obtained at $\varepsilon = 0.05$ and yield point behavior for an aluminum-3.5% magnesium alloy in reference (29). Al-Haidary *et al.* provided near-parabolic curves for the $\sigma_{0\varepsilon}$ dependencies of all three materials at ambient temperature and 200 °C and gave an interpretation of the results in terms of the dislocation density, ρ, that may be tracked to the original theory of Taylor (4) and expectation of a parabolic $\sigma_\varepsilon - \varepsilon$ curve but with $\sigma_{0\varepsilon}$ replacing σ_ε (46). The addition of the $k_\varepsilon \ell^{-1/2}$ term provided evidence that slip transmission across grain boundaries continued to be required during plastic straining. At higher temperatures, evidence was provided of dislocation annihilation occurring and, at lower temperatures, transition occurred to a linear dependence on ρ and subsequent hardening due to the difficulty of cross-slip. Ogilvie and Boas had first reported cross-slip occurring in aluminum at the time of its originally being reported to occur in surface slip step height observations made on deformed α-brass by Maddin, Mathewson and Hibbard (47).

Dorn has reported on interpretation of the low temperature deformation properties of aluminum and related metals and alloys in terms of thermally-activated dislocation migration and including, among a number of issues, characterizations of dislocation intersections, solute strain centers and cross-slip (48). Such important influence of temperature (and strain rate) enters largely into the $\sigma_{0\varepsilon}$ dependence that has been elaborated also on a dislocation mechanics basis by Zerilli and Armstrong (49, 50) in the so-called Z-A relations:

$$\sigma_\varepsilon = \sigma_{0G\varepsilon} + B\mathbf{exp}[-\beta T] + B_0[\varepsilon_r(1 - \mathbf{exp}\{-\varepsilon/\varepsilon_r\})]\mathbf{exp}[-\alpha T] + k_\varepsilon \ell^{-1/2} \qquad [3]$$

In Eq. (3), $\sigma_{0G\varepsilon}$ is an athermal stress dependent on the dislocation density, subgrain structure and solute, and B, β, B_0, ε_r, and α are experimental constants that are physically based in dislocation mechanics. The second and third terms on the right-side of the equation are derived from a thermal activation influence, $\sigma_{Th\varepsilon} = \sigma_\varepsilon - [\sigma_{0G} + k_\varepsilon \ell^{-1/2}]$, on the material yield stress and strain hardening, respectively. Equation [3] is expressed in a general form potentially applicable to both fcc and bcc metals and alloys; some hcp metals, such as magnesium, zinc, and cadmium follow an fcc-like behavior while others, such as alpha-titanium, zirconium and hafnium follow a bcc-like behavior. The strain rate dependence, $d\varepsilon/dt$, is obtained from the (β, α) parameters that follow a weaker dependence:

$$(\beta, \alpha) = (\beta_0, \alpha_0) - (\beta_1, \alpha_1)\mathbf{ln}(d\varepsilon/dt) \qquad [4]$$

The first three terms on the right side of Eq. [3] are normally combined in $\sigma_{0\varepsilon}$. In contrast with the bcc case for which the temperature and strain rate dependence is in the (second term) yield stress, these dependencies for fcc metals are principally in the strain-hardening. As a consequence, $B = 0 = \beta_0 = \beta_1$ thus leading to the simplified fcc relation:

$$\sigma_\varepsilon = \sigma_{0G\varepsilon} + B_0[\varepsilon_r(1 - \mathbf{exp}\{-\varepsilon/\varepsilon_r\})]\mathbf{exp}[-\alpha T] + k_\varepsilon \ell^{-1/2} \qquad [5]$$

The second term on the right side takes account of dislocation annihilation, as described by Al-Haidary *et al.*, and of dynamic recovery that leads to a lessor increase in dislocation density, ρ, than described in the Taylor model (50). At small strains, the term approximates to the Taylor parabolic $\varepsilon^{1/2}$ dependence.

Equation [5] has been used to describe extensive measurements reported for copper materials (49). Zerilli and Armstrong had given an estimation of several of the Z-A temperature parameters for aluminum (51). Other constants have been given for AA7075-T6 material (52) and for a modified Z-A relationship (53). The weaker strain rate dependence indicated in Eq. [4] increases for very high rate loading in shock impact tests and for comparable strain rates achieved in *shock-less* isentropic compression tests.

Shock and *Shock-less* Isentropic Compression Experiments

The Z-A equations were developed principally to describe high rate deformations such as impact and leading to shock loading and equivalent strain rates in *shock-less* isentropic compression experiments (ICEs). Huang, Asay and colleagues have investigated such conditions for ultrapure aluminum (99.9998 %) and for various aluminum alloys including polycrystalline and single crystals (54-56). Yield stress measurements as high as 90 GPa were reported but without indication of H-P dependence (54). Follow-up comparison in tests on single crystal and polycrystal material confirmed the lack of H-P dependence (55). Additional high pressure measurements on aluminum under quasi-isentropic compression generated higher yield stresses (56).

Armstrong, Arnold and Zerilli have reported on both shock and ICE types of very high rate loading and pointed to the different considerations of dislocation generation being important at a propagating shock front as compared with dislocation drag resistance controlling migration of the resident dislocation density in shock-less isentropic compression (57). Experimental results on Armco iron and copper were analyzed. An H-P dependence was determined for the shock-induced Hugoniot elastic limit stress, σ_{HEL}, determined by deformation twinning for Armco iron. The subsequent value of σ_{ε}, found to be independent of grain size, was explained in terms of the plastic deformation being necessarily accommodated at the much smaller nano–scale points all along the propagating shock front. For equivalent strain rates reached in shock-less ICEs, a different situation occurs of the uniformly rising compressive stress driving the resident dislocation population at such extreme velocity as to be retarded only by the crystal lattice determined dislocation drag. Higher stresses are required.

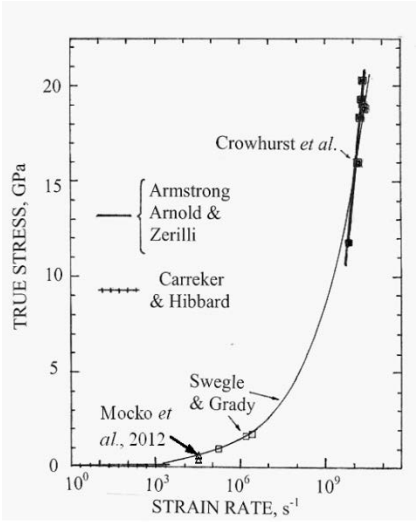

Figure 6. Strain rate dependence of shock-induced plasticity.

Figure 6 shows experimental measurements and predictions obtained on aluminum materials (31, 57-60). The previously mentioned strain rate dependent results obtained by Carreker and Hibbard are superposed on the abscissa scale at the lowest strain rates. Moćko, Rodriguez-Martinez, Kowalewski and Rusinek reported split-Hopkinson pressure bar results obtained on commercial AA 7075-T6 material for which the strain rate dependent $\Delta\sigma_\varepsilon$ measurements are plotted in Fig. 6 (58). Swegle and Grady had reported pioneering measurements on aluminum material that followed the indicated power law relationship drawn in the figure (59). The highest stress results by Crowhurst et al. (60) have been fitted to a linear dependence predicted as a limiting case of the Z-A analysis (57). Malygin, Ogarkov and Andriyash have provided a dislocation model description of shock wave results obtained on aluminum and related materials (61). Gurrutxaga-Lerma, Balint, Dini and Sutton (62) have reported elastodynamic model calculations of the strain rate dependence leading to homogeneous dislocation generation in aluminum.

H-P dislocation pile-up model

Both Hall and Petch attributed the inverse square root of grain size dependence exhibited for the yield and cleavage strength measurements made for their steel materials to the dislocation pile-up model proposed at about the same time by Eshelby, Frank and Nabarro (63). In the review by Armstrong (35), a value of $k = 23.4$ MPa.mm$^{1/2}$ was reported for the pronounced lower yield point behavior of mild steel at ambient temperature. A lessor $k_{.10} = 12.4$ MPa.mm$^{1/2}$ was determined for the H-P flow stress dependence, thus indicating by the reduction in value that a high k_{lyp} is associated with a pronounced lower yield point stress determined by carbon locking of dislocations in the grain boundary regions, such as depicted in Fig. 2. Zener had proposed earlier that such pile-ups, analogously associated with a model of a shear crack impinging on a grain boundary, were responsible for the yield stress dependence on reciprocal square root of grain size of brass material (64) and for the mechanism of cleavage fracturing of steel (65). Li and Chou produced a seminal description of dislocation pile-up characteristics (66). Armstrong has given a later review of the dislocation pile-up model equations for the H-P dependence (67).

Analogous Pile-Up/Shear Crack Description

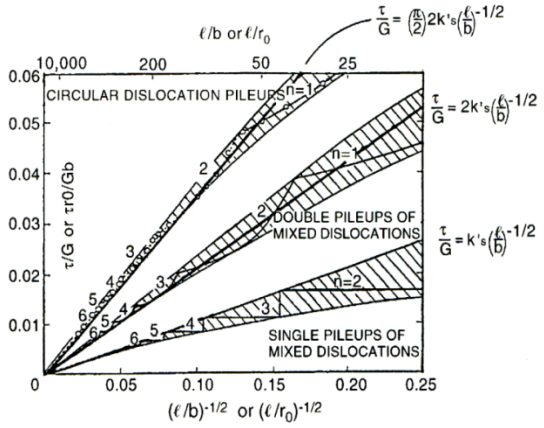

Figure 7. Comparison of dislocation pile-up and crack size predictions (67).

In the pile-up model description, $k_{S\varepsilon}$ is described as a microstructural shear stress intensity, analogous to the macroscopic stress intensity specified in the fracture mechanics of pre-cracked materials (68). Figure 7 illustrates an example connection between the H-P calculations for a single-ended, double ended, and circular pile-up geometry and the counterpart fracture mechanics equations for an edge crack, internal crack, and circular crack geometry. In the figure, $r_0 \approx b$ is a dislocation core radius. At small grain sizes or crack sizes, the figure shows that there is divergence from a continuum description of the crack size dependence as compared with the discontinuous pile-up equation descriptions that are quantized in terms of b or r_0. As will be seen, such consideration becomes important at the limiting strength properties to be described for nano-scale grain size material.

Far lessor k_ε values are measured for plastic yielding, as expected, compared with the cleavage $k_C \approx 100$ MPa.mm$^{1/2}$ obtained for the low temperature fracturing of iron and steel materials. For general yielding and subsequent plastic flow, the pile-up model for an ideal slip band provides for evaluation of $k_\varepsilon = m_T k_{S\varepsilon}$ in terms of the local shear stress, τ_C, on the lead dislocation in a pile-up (30) as

$$k_\varepsilon = m_T[\pi m_S G b \tau_C / 2\alpha']^{1/2} \qquad [6]$$

In Eq. [6], m_T and m_S are the Taylor and Sachs orientation factors mentioned above, G is the elastic shear modulus, b is the dislocation Burgers vector, and $\alpha' = 2(1 - \nu)/(2 - \nu) \approx 0.8$ is an average factor for a screw or edge dislocation character. On this basis, then, the H-P pile-up model description leads to two shear stresses controlling polycrystalline plasticity: $\tau_{0\varepsilon}$, for the average 'friction' shear stress for dislocation movement within the grain volumes; and, τ_C, for the local stress gauging the obstacle resistance to transmission of plastic flow across the grain boundary. Two reasons for k_ε being relatively large are τ_C being higher for the yield point associated 'dislocation locking' in the grain boundary region, as indicated schematically in Fig. 2 (29, 69), and for the combined reasons of m_T, m_S and τ_C being large for secondary slip or twinning systems to operate in the grain boundary regions. The former effect is best illustrated by steel for which the H-P relation was initially established and the latter effect is particularly important for hcp metals and alloys that generally show intermediate k_ε values between those of bcc and fcc metals (29, 70). A k_{HP} dependence on carbon segregation at grain boundaries, as in Fig. 2, has been recently reported even in the fcc case of a high manganese austenitic steel (71).

Aluminum H-P k_ε Determined by Cross-Slip

The importance of (post-Taylor) cross-slip to understanding the deformation and strain hardening behaviors of fcc metals led to the notion that cross-slip could be responsible for determining the value of k_ε in pure fcc metals (40), especially because of association between the low k_ε value for aluminum and its ease of cross-slip. An absence of easy glide and early onset of cross-slip in an aluminum single crystal allowed Taylor to match the deformation curves of single crystal and polycrystalline aluminum. Bell provided a later compilation of cross-slip shear stresses, τ_{III}, in aluminum and in other fcc single crystal deformation results relating to the fit of Taylor-type parabolic strain hardening (72). A critical review of the important cross-slip deformation mechanism associated with strain rate effect, hardening, recovery, and microstructural evolution has been given by Pùschl (73). Alankar, Field and Zbib have incorporated the mechanism into a model for the development of dislocation densities in single crystals (74).

Figure 8 provides a schematic description of cross-slip occurring in the aluminum bi-crystal experiments of Clark and Chalmers (9, 75). Cross-slip of dislocations at the pile-up tip is proposed to establish a limit on the critical value of τ_C specified in Eq. [6]. Of course, $\tau_{III} > \tau_{0\varepsilon}$ for most single crystal test orientations.

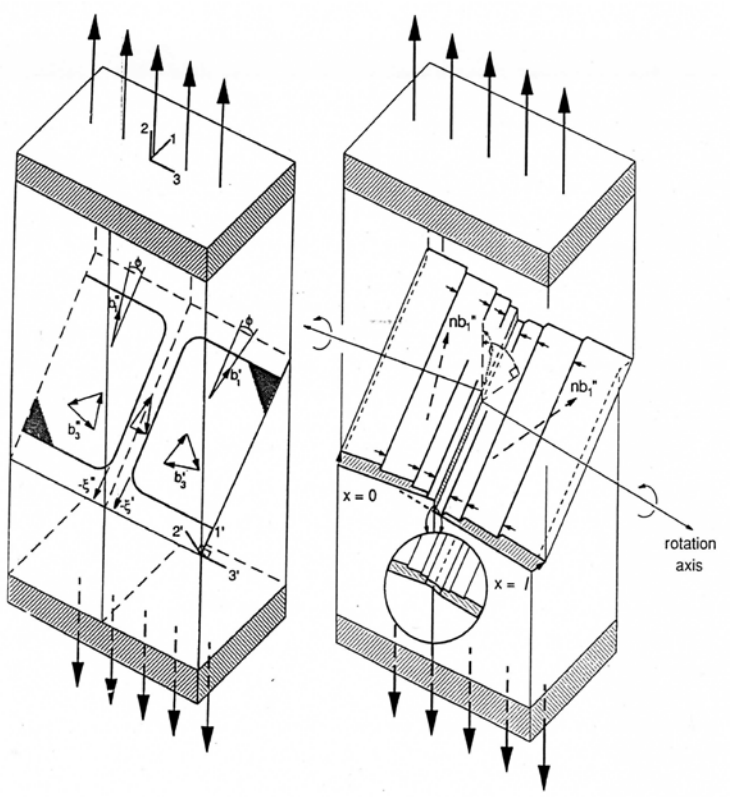

Figure 8. Model for cross-slip in an aluminum bi-crystal deformation experiment (9, 74).

An early comparison (40) had been made for aluminum and copper of similar temperature dependencies for their cross-slip shear stresses, τ_{III}, (72, 76) and k_ε^2 values (41, 77) compiled from reported data. Likewise, similar strain rate dependencies were established for copper τ_{III} and k_ε^2 values (78). Such prediction had been established earlier for H-P measurements reported for (hcp) magnesium material in which $\sigma_{0\varepsilon}$ was shown to follow the same temperature dependence as that for the basal slip resolved shear stress, $\tau_{(0001)<11\text{-}20>}$, and k_ε^2 was shown to follow the same temperature dependence as for the resolved shear stress for the prism slip system, $\tau_{\{10\text{-}10\}<11\text{-}20>}$ (79).

Metal	Shear modulus (GPa)	Burgers vector (nm)	τ_{III} (MPa)	Theoretical k_ε (MPa.mm$^{1/2}$)	Experimental k_ε (MPa.mm$^{1/2}$)
Al	25	0.29	4.5	1.2	1.5
Ni	62	0.25	17	3.3	4.9
Cu	30.5	0.256	29	3.1	5.0
Pb	4.8	0.35	1.6	0.33	0.43

Table I. Comparison of H-P Predicted and Experimental k_ε Values.

More recently, the prediction of ambient temperature values of k_ε values determined from Eq. [6] have been compared with experimental measurements. Table 1 provides such comparison for aluminum (33), nickel (80), copper (43) and lead (81) materials. The experimental k_ε values compare very favorably with those tabulated by Hansen (82).

H-P Application to Aluminum Alloys

An important review of early 20th century development of aluminum alloy technology was given by Dean (83) in an article giving great credit to very relevant metallurgical contributions of Zay Jeffries; see also for example the pioneering reference to Jeffries on grain size effects in metals (84). Dean described pioneering contributions made by Jeffries on: aluminum alloy casting technology, particularly Al-Si and Al-Si-Cu alloy developments; aluminum alloy thermal expansion properties; beneficial microstructural refinement *via* high solidification rates; heat treatment for solid solution strengthening and 'aging' for atomic clustering/precipitation strengthening; and aluminum alloy development for forging operations. Interesting connection on the importance of thermal expansivity in aluminum alloy developments may be seen in reported measurements of local plasticity produced by cyclic thermal straining of Al-Si alloy and other composite materials (85, 86). A recent report has been given by Czerwinski, Kasprzak, Sediako, Emadi, Shaha, Friedman and Chen on high temperature Al-Si-Cu-Mg base alloys with Zr, V, and Ti micro-additions successfully developed for automotive power trains (87).

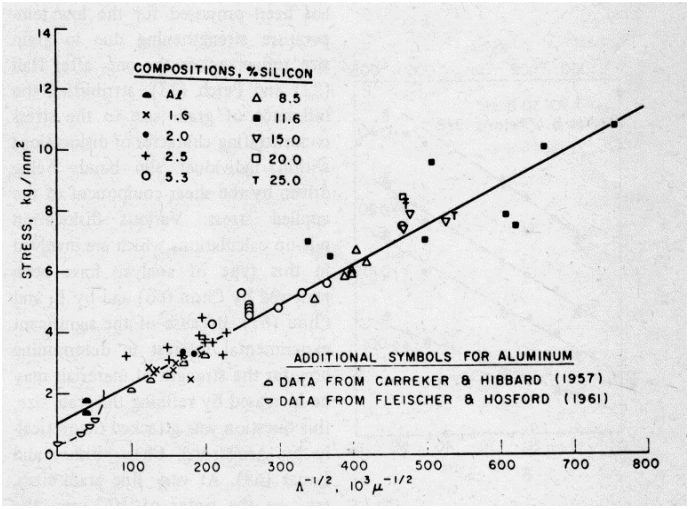

Figure 9. Extended H-P application to yield strength of Al-Si alloy materials (88).

Figure 9 shows application by Erginer and Gurland of the H-P model description to yield stress measurements made for Al-Si alloy materials in which the two-phase (intercept) mean free path length, λ, has been substituted for the average grain diameter, ℓ (88). The grain size determined H-P results of Carreker and Hibbard (31) and specimen size affected results of Fleischer and Hosford (32), shown in Fig. 3, are plotted near to the origin of the current figure that also indicates thereby a same value of $k_\varepsilon \approx 2.5$ MPa.mm$^{1/2}$. Liu and Gurland had indicated a same type result for higher carbon spheroidized steel materials (89). Morrison and Leslie had demonstrated analogous type result for lower carbon steel materials (90). Thus, one aspect of alloy strengthening caused by precipitates is to effectively refine the

microstructural scale. Earlier, Ansell and Lenel had proposed an inverse square root dependence for the yield strength dependence of dispersion strengthened, sintered aluminum powder material (91).

H-P for Solid Solution Strengthened Alloys

Suzuki and Nakanishi reported H-P measurements for Cu-Al and Cu-Ni alloys (92) and then presented a detailed dislocation pile-up model description for the H-P dependence of the yield stress for fcc alloy materials (93). Measurements of greater k_ε values for the two alloys and also Cu-Zn materials were interpreted in terms of the alloy solute segregating in the grain boundary region analogous to the situation for carbon in steel; see Fig. 2. Very interestingly, a smallest increase in k_ε occurred for the Cu-Ni system for which nearly the same k_ε values are measured for each one of the pure materials; see Table I. Mention was made of the temperature dependence for the Cu-Al k_ε being the same as that for copper; this relating to the mentioned account (77) of k_ε^2 following that for the cross-slip shear stress, τ_{III}. Other direct application of an H-P description to yield stress measurements made on several Al-Mg solid solution alloys is shown in the compiled results of Fig. 10 (94) including the pure aluminum result and H-P temperature dependence for Al-2-25 Mg (45). Results on Al-Li and Cu-Zn (brass) alloy materials were also presented (94).

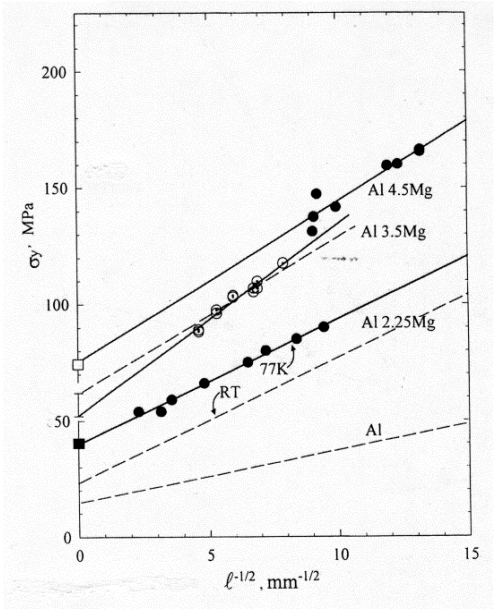

Figure 10. Compiled H-P dependencies for Al-Mg alloys (94).

Other H-P connection has been made for textured Al-Li 2090-T8E41 alloy relating to its very significant anisotropic plastic deformation and cracking behavior associated with both a laminated grains exhibiting a crystallographic texture (75). The material is a candidate for the structural application in the aerospace industry. The surface structure of a residual macro-indentation was employed to demonstrate the plastic anisotropy of the elongated grain structure. Microscopic grain boundary protrusions into the residual circumferential crater were taken to demonstrate grain size strengthening in an analogous manner to that described by Polanyi (2). Delamination type cracking was described for dislocation pile-ups reactions based on the material having an ideal copper or brass texture. A later report has been made by Tayon, Crooks, Domack, Wagner and Elmustafa has related the delamination cracking to orientation variants of a

brass texture (95). The fracturing was attributed to “a lack of slip accommodation across the [grain] boundary, which promotes significantly higher deformation in one grain and, and stress concentrations that promote delamination …”.

Serrated Plastic Flow

The strong grain size dependence associated with serrated plastic flow in metal alloys has been reviewed by Antolovich and Armstrong (96). Original deformation curves reported for an Al-Cu-Mn alloy in 1923 by Portevin and Le Chatelier (97) and in 1949 on a commercial aluminum material by McReynolds (98) were reproduced in the review. Cottrell had explained the PLC behavior in terms of sequential dynamic interaction of diffusing substitutional solute with deformation-induced dislocation migration (99) but, until the present time, little attention has been given to the importance of a substantial grain size dependence of the behavior relating to an H-P dependence. There is an important strengthening effect at lower strain rate because of the behavior that is analogous to the strain aging behavior observed for carbon in steel. Wagenhofer, Erickson-Natishan, Armstrong and Zerilli investigated the strain rate and grain size dependent behavior for the commercial Al-4 wt. % Mg alloy 5086, also containing 0.4 wt. % Mn and 0.15 wt. % Cr (100). Figure 11 shows a comparison of the higher flow stress measurements made on as-received material in an H-32 cold-worked and proprietary recovery treatment as compared with the material in a (lower stress) fully-annealed condition and with Al-4.5 Mg results and pure aluminum material. Serrated flow was observed for example at a strain rate of 10^{-3} s^{-1} and an absence of serrations was observed for a lower flow stress at a higher strain rate 0.36 s^{-1}. The increased strengthening at lower strain rate was compared with very high rate loading measurements and a Z-A model description of them. The PLC behavior is a particularly important research topic in current investigations of nickel superalloy materials (101).

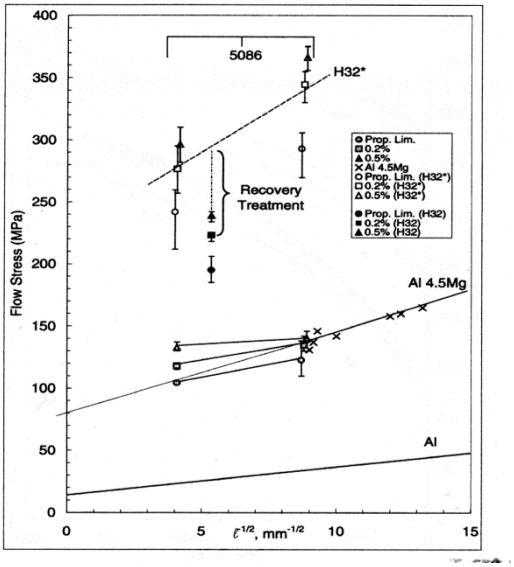

Figure 11. H-P dependencies for Al 5086 alloy material (100).

Ultrafine to Nano-Scale Grain Sizes

Extension of the conventional H-P measurements to nano-scale grain sizes of steel materials gave indication that increases of yield and fracture stresses would occur by an order of magnitude in the $k_\varepsilon \ell^{-1/2}$ term; see Table I in (102). An H-P dependence was demonstrated for nanocrystalline aluminum by Bonetti, Pasquini and Sampaolesi (103). Mukai and Hugashi reported ductility enhancement measured for an Al-14 wt%-14wt% Mn alloy that followed an H-P dependence and was produced by crystallization of amorphous powers by hot extrusion (104). Hokka, Kokkonen, Seidt, Matrka, Gilat and Kuokkala have reported high rate torsion results for ultrafine-grained 1070 aluminum material (105) and Khan, Suh, Chen, Takacs and Zhang demonstrated strain rate dependent plasticity for nanocrystalline aluminum in dynamic loading tests (106). The combined issues of structural morphology, boundary spacing, boundary mis-orientations and dislocation density were described for nanostructured aluminum by Huang, Kamikawa and Hansen (107). Bazarnik, Huang, Lewandowska, and Langdon reported H-P behavior for an Al-5Mg alloy processed by the method of high pressure torsion (108).

Meyers, Mishra and Benson had produced an earlier comprehensive review of mechanical properties for nanocrystalline materials (109). Li edited an important book on the topic (110). Armstrong produced a recent review article (111). Figure 12 shows a comparison of conventional and nano-scale H-P results plotted on a log/log scale for aluminum, copper and nickel materials. On such log/log basis, a relatively constant value of $\sigma_\varepsilon = \sigma_{0\varepsilon}$ is approached at large grain sizes and a linear slope of -1/2 is approached at very small grain sizes. In Fig. 12, the conventional grain size (open symbol) measurements have been referenced already for aluminum (31), copper (43), and nickel (38). The nickel results, shown at a relatively larger strain of $\varepsilon = 0.14$ with accompanying $k_{.14} = 2.15$ MPa.mm$^{1/2}$, had been achieved after an initial value of $k_{.002} = 5.17$ MPa.mm$^{1/2}$was measured. The nickel measurements show an essentially constant value of $k_\varepsilon \approx 5$ MPa.mm$^{1/2}$ (112), very near to the same value as obtains for copper (43); see Table I. The reason for the same initial k_ε values is attributed to the product, $G\tau_C = G\tau_{III}$ in Eq. (6), thus compensating for a two-times increase in G for nickel by a reduction of approximately one-half in τ_{III}.

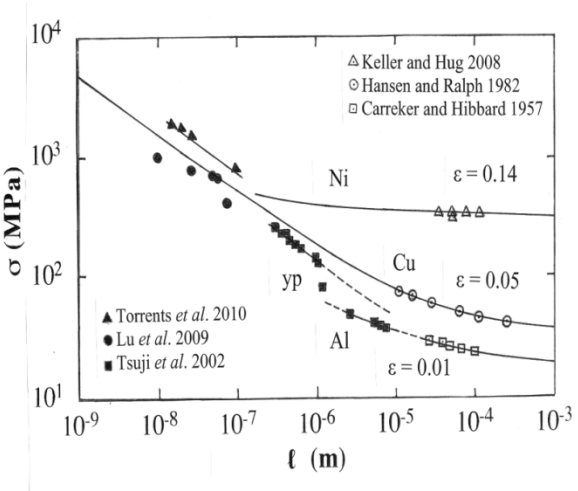

Figure 12. Conventional and nano-scale H-P results for Al, Cu and Ni (111).

The ultrafine grain size measurements for aluminum, copper and nickel materials were compiled from results reported, respectively, by Tsuji, Ito, Saito and Minamino (113); L. Lu, Chen, and K. Lu (114); and

Torrents, Yang and Mohammed (115). In Fig. 12, the finer grain size measurements for aluminum showed a relatively larger k_ε = ~3.5 MPa.mm$^{1/2}$ at larger grain size then increasing to ~4.5 MPa.mm$^{1/2}$ at smaller grain sizes in which a significant yield point behavior was also observed. Such larger k_ε associated with yield point behavior relates to the earlier-mentioned results for austenitic steel (71). The transition to the stronger grain size dependence occurred also at the point of the yield stress becoming equal to the ultimate tensile stress. The yield stresses for the ultrafine grain size measurements are shown to increase by an order-of-magnitude or more for aluminum and copper, and this is also true for nickel when compared on a yield stress basis. Recent report has been of precipitate and grain boundary influences on strength levels reached above 1.0 GPa and plastic stability of sub-micron aluminum micro-pillars (116).

Thermal Activation in k_ε

The value of τ_C in Eq. (6) provides for the possibility of thermal dependence in accordance with the Z-A description given in Eqs. (3) – (5), with proviso that τ_C is not too large (81). The k_ε values have been demonstrated to be thermally activated, first, for the hcp metals (117, 118) and then for fcc metals (40). As a consequence, the shear strain rate sensitivity parameter, $v^* = k_B T[\partial \ln(d\gamma/dt)/\partial \tau_{Th\varepsilon})]_T$, with k_B being Boltzmann's constant, takes on an H-P type grain size dependence from Eqs. (3) and (6) given by the relationship

$$(1/v^*) = (1/v_0^*) + (k_\varepsilon/2m_T\tau_C v_C^*)\ell^{-1/2} \qquad (7)$$

In Eq. (7), v_0^* is the activation volume determined from strain rate influence on $\sigma_{0\varepsilon}$ and the H-P dependence follows from the thermal product, $\tau_{ThC}v^*_C$ being constant (40, 119) and so long as the athermal component of τ_C, that is τ_{GC}, is not too large. Figure 13 shows connection of conventional grain size nickel measurements of Narutani and Takamura (112) made by Armstrong and Rodriguez (120) to a combination smaller grain size measurements for copper and nickel materials compiled by Asaro and Suresh (121) and, also, with mixed-in nickel measurements reported by Weng (122), and with copper measurements reported by Lu et al. (114) for nano-twinned material taking the twin spacing, λ, as the effective grain size. The two solid Eq. (7) curves are predicted for 195 and 300 K (120).

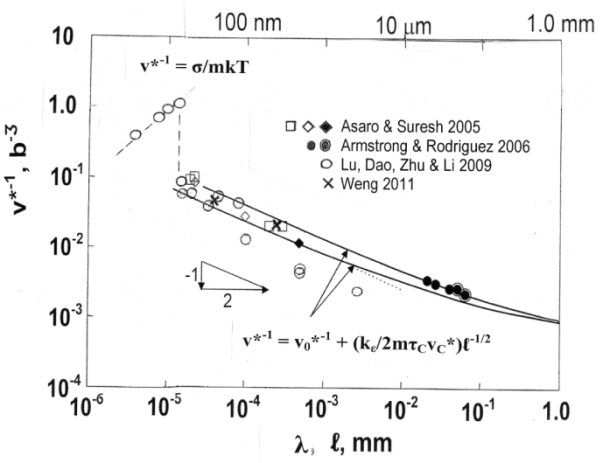

Figure 13. A reciprocal activation volume dependence for Ni and Cu materials.

Similar strain rate dependent nanoindentation hardness measurements made for conventional and ultrafine grain size Al 99.5 material, as those shown on the right side of Fig. 13, were obtained by May, Höppler and Göken (123), as reported by Meyers et al. (109). The strain rate sensitivity measurements in this case were reported in terms of the parameter, $m = [\partial \mathbf{ln}(d\varepsilon/dt)/(\partial \mathbf{ln}\sigma)]_T$. A constant value of m was found over a range of strain rate for both grain sizes that, for the ultrafine grain size material, was from 10^{-3} to 1.0 s^{-1}. With the hardness, $H \approx 3\sigma_\varepsilon$, a value of v* is obtained as

$$v^* = 3k_BT/mH \tag{8}$$

On such basis, v* for the conventional grain size material gave relatively constant higher values in the range ~80 to ~70 b^3 as compared with the ultrafine grain size material giving a smaller value of v* decreasing with increasing strain rate from ~11 to ~8 b^3, in both cases decreasing with increasing strain rate. The trend of the aluminum v* values are consistent with those shown for copper in Fig. 13.

Grain Size Weakening

At the smallest λ values shown in Fig. 13, a reversed H-P dependence was reported for σ by Lu et al. (114) as indicated in the top-left corner of the figure and accounted for in terms of constitutive equation behavior at higher temperatures (68). For this case, which behavior is generally observed for $\ell \leq$ ~20 nm, there is grain size weakening similar to that observed at very high temperatures of grain boundary shearing and diffusive deformations occurring more easily than transgranular slip or twinning (84, 124). Balusubramanian and Langdon had reported creep-connected superplastic flow for an equal-channel angular pressed (ECAPed) sub-micrometer Al-Mg-Sc alloy material for which grain boundary sliding was proposed to be accommodated by intragranular flow of dislocations (125). The same authors have produced a more recent review covering superplastic flow observed for a compilation of aluminum- and magnesium-based alloys as well demonstrating appreciable Hall-Petch based strengthening at nano-scale grain sizes (126). Presumably for the weakening aspect of such limiting nano-scale material, the H-P induced very high stress state brings into play localized shear deformations within the grain boundaries. Pande and Cooper have provided an important review of the limiting transition to nanoscale weakening behavior (127). Mompiou, Legros, Boé, Coulumbier, Raskin and Pardoen have provided important *in-situ* TEM tensile test observations of intergranular dislocation motion in the grain boundary plane of aluminum thin film material and provided comparison with their own measurements of transgranular plasticity (128). Padmanabhan, Sripathi, Hahn and Gleiter have reported on their own model description of grain/interphase boundary sliding as applied to reported measurements of an inverse H-P effect in Al-Cu-Fe nanoquasicrystalline alloy and nanocrystalline Zn and Ni materials, including the prediction of superplastic flow (129). Kong and Fang have produced an important review of grain boundary relaxation measurements first observed in internal friction measurements made on polycrystalline aluminum at above ambient temperatures and now including vertical bi-crystal boundaries, as in Fig. 8, along with limited results reported thus far on ultrafine grain size materials (130).

Tensile Plastic Instability, Fracturing and Fatigue

Important research results have been obtained on aluminum materials that again serve to elucidate a similar range in the broader aspect of material properties including topics of tensile instability, shear banding, ductile fracturing and fatigue behavior. Because of its low H-P microstructural stress intensity, k_ε, value, aluminum doesn't show any remarkable tensile instability behavior other than providing, in line with normal fcc type constitutive behavior, a greater uniform true strain to maximum load at greater strain rate (131) and a minor susceptibility to shear banding behavior (132).

Tensile Instability/Fracturing

Figure 14 shows an important comparison of H-P yield stress measurements (open triangles and circles) and true stress at maximum load values (closed circles) for accumulatively roll-bonded (ARB) and annealed high-purity aluminum material able to be obtained from very complete measurements reported by Kamikawa, Huang, Tsuji and Hansen (133). The larger grain size open triangle points were obtained for cold-rolled and annealed material. The smaller grain size, paired circle A, B, C, and D points, were associated with significant H-P strengthening from the outset of straining but with appreciably reduced uniform strain leading to rapid onset of plastic instability, compared to the larger grain size points E and F that showed extended strain hardening until reaching the plastic instability stress.

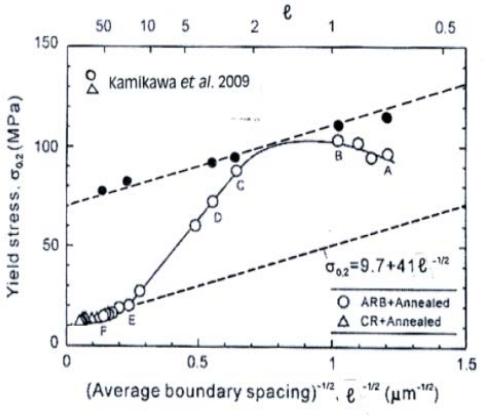

Figure 14. Yield and maximum true stress for accumulative roll-bonded (ARB) Al.

Basinski had produced a pioneering analysis of tensile instability as related to the onset of shear banding in pure and commercial aluminum materials tested at 4.2 K (134). No account was made of grain size influence until Chin, Hosford and Backofen showed an H-P dependence for their own fracture stress measurements also made at 4.2 K (135). An evaluation of the aluminum measurements was made as part of a comparison with steel material yield-to-fracture strength measurements (136). On an H-P basis, the aluminum ductile fracture stress gave σ_{0F} = ~540 MPa and k_F = ~54 MPa.mm$^{1/2}$. The value of k_F was found to be two times larger than a theoretical brittle fracture stress value employing the theoretical true surface energy measurement thus giving very significant evidence of plastic flow on cracking even at 4.2 K. Lassance, Fabrègue, Delannay and Pardoen have reported on the micromechanics of ambient and higher temperature fracture of 6xxx aluminum alloys (137). More recently, a comprehensive report has been made by Khadyko, Myhr, Dumoulin and Hopperstad on the importance of texturing in the 6xxx alloys, particularly concerning the influence of alloying elements in solid solution and as precipitates, on the corresponding yield stress and strain hardening behaviors (138). Valuable references to historical

measurements dating to the early twentieth century researches of Taylor and Elam are included. Shakoori Oskooie, Asgharzadeh and Kim have reported on achievement of reasonably high strength and ductility in Al-Mg-Si Al6063 alloy with a bimodal ultrafine grain and coarse grain structure (139). Very interestingly, tensile fracturing was attributed to elongated-hole delamination from internal necking of the coarse grain component, somewhat similar to a description of the true fracture strain attributed to hole-joining from de-cohered particles in a ductile fracturing model developed by Petch and Armstrong (131).

An H-P based explanation has been given of the minor amount of shear banding that occurred under the circumstance even in the Basinski case of such low temperature testing (140). In a broader situation, the onset of shear banding has been attributed to the occurrence of dislocation pile-up avalanches in materials exhibiting high values of the microstructural stress intensity, k_ε (141). Figure 15 shows on the basis of the inset pile-up avalanche equation, a prediction of susceptibility to shear banding measured by the slopes of lines to coordinate points of theoretical shear fracturing, k_S, versus thermal conductivity, K*, for a number of metals (142). The difficulty of producing shear banding in aluminum may be compared with the well-known susceptibility of shear banding in Ti6Al4V material. Shear strain localization measurements have been recently reported for AA 2219-T8 aluminum alloy in split-Hopkinson compression bar tests at high strain rates in which cracking occurred along the shear bands and was associated with dispersed second phase particles (143).

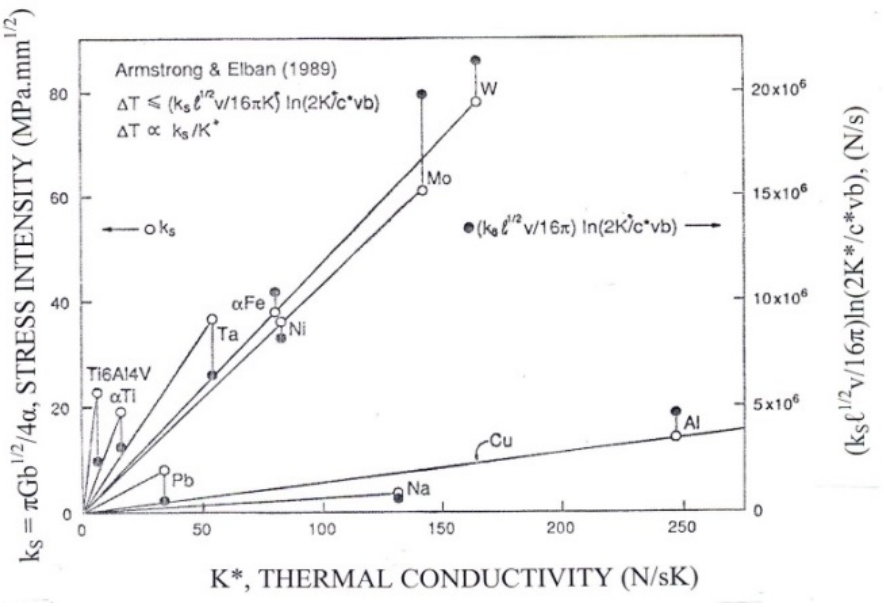

Figure 15. H-P dislocation pile-up avalanche model for shear banding.

Fatigue

As mentioned above, Gough had produced pioneering comments on the fatigue behavior of aluminum multi-crystals in the 1928 Faraday Society Proceedings (3). Aluminum occupies a unique position in development of aerospace technology. Forsyth, Stubbington and Royal Aircraft Establishment colleagues produced a breakthrough description of slip-band extrusions developed on the surface of pure aluminum

material under cyclic loading (144, 145). Cottrell and Hull reported observations of both extrusions and intrusions produced by cyclic slip in copper tested at temperatures as low as 4.2 K (146). The observations built onto the original description by Thompson, Wadsworth and Louat of cyclically-induced persistent slip bands (PSBs) in copper (147). Figure 16 shows connection of surface structure, dislocation (pile-up) activity and dipole formation as developed under cyclic stress conditions (148). Broom, with Whittaker, also first described an important role for generation of vacancies and enhanced diffusion mechanisms for effecting over-ageing behavior in aluminum alloy systems (149) and then added comment on cross-slip being an important mechanism in effecting fatigue (150).

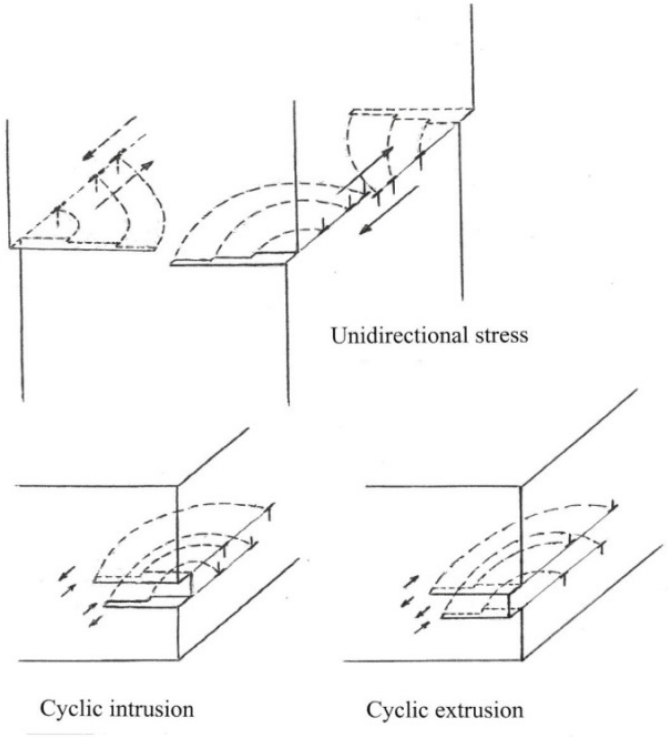

Figure 16. Schematic surface extrusion/intrusion and internal dislocation structure.

Armstrong and Phillips reported on specimen size and H-P based grain size effects in compiled measurements made on α-iron, low-carbon steel and α-brass materials (151), to be followed by compilation of other H-P description of comparative brass results (21). Turnbull and de Los Rios produced H-P measurements made of an endurance limit in commercially pure aluminum material and attributed the dependence to the grain boundaries providing barriers to dominant crack growth (152). Agreement between cyclic stress strain measurements and H-P grain size effect was reported for other aluminum material by El-Madhoun, Mohamed and Bassim (153). The nature of PSBs in a number of commercial aluminum materials was modeled by via finite element description by Baxter and Wang (154). Emphasis was given to PSB behavior being more important than crack growth consideration. Zhang and (Z.G.) Wang produced an important review of grain boundary effects on the cyclic stress-strain curve and fatigue damage with assertion that interaction of PSBs and grain boundaries played a decisive role in intergranular fatigue cracking (155). In line then with expectation for ultrafine grained

material, an overview has been given of specific improvements in fatigue behavior produced by equal-channel angular pressing ECAP of copper, aluminum, AA6061 alloy, and α-brass materials (156). The results are in agreement with the general description made later of H-P based grain size reduction providing improved fatigue properties for other ultrafine-grained copper material (157, 158). Valiev, Estrin, Horita, Langdon, Zehetbauer and Zhu have reported most recently on the very significant advances being made on production via severe plastic deformation of bulk ultrafine-grained aluminum alloy and other materials with outstanding improvements in strength and ductility (159).

SUMMARY

The plastic deformation and ductile fracturing properties of aluminum and certain aluminum alloys have been reviewed with particular attention given to the use of a Hall-Petch description of grain size aspects of the material behaviors. Initial focus is on the historical role of aluminum in having provided important support for the Taylor theory of dislocation-effected metal plasticity. Microstructural aspects of polycrystalline grain, subgrain, and grain boundary features have been described, especially in the direction of pointing to important strengthening effects at nano-scale grain sizes. An interpretation of the H-P dependence of strength property measurements is provided on the basis of a dislocation pile-up representation of slip bands forcing cross-slip at aluminum and other pure fcc metal grain boundaries. Measurements of temperature, and strain rate influences are described in terms of additional relationship to the physically-based Zerilli-Armstrong relations that have been developed from a dislocation mechanics description of thermally-activated plasticity, including shock-induced deformation and description of comparable deformation rates achieved in *shock-less* isentropic deformations. Measurements are presented for a number of aluminum alloys. Grain size aspects of strain ageing, tensile plastic instability, shear banding, ductile fracturing and fatigue properties have also been reviewed.

References

(1) Taylor, G.I.; Resistance to shear in metal crystals. Trans. Farad. Soc. 1928, 29, 121-125.
(2) Polanyi, M.; Deformation, rupture and hardening of crystals. Trans. Farad. Soc. 1928, 29, 72-83; Discussion, 172.
(3) Gough, H.J.; Note on some fatigue phenomena with special relation to cohesion problems, Trans. Farad. Soc. 1928, 29, 137-148.
(4) Taylor, G.I.; The mechanism of plastic deformation of crystals. Part 1.-Theoretical. Proc. R. Soc. Lond. 1934, 145, 362-387.
(5) Taylor, G.I.; Plastic strain in metals. J. Inst. Met. 1938, 62, 307-324.
(6) Kocks, U.F.; The relation between polycrystal deformation and single-crystal deformation. In Deformation and Strength of Polycrystals, Fall Meeting of TMS-AIME, Detroit, MI, October 14, 1968; Armstrong, R.W.; Feltner, C.E., Eds., Metall. Trans. 1970, 1, [5], 1121-1143.
(7) 'Orange Peel'; Tech Notes. Adv. Mater. & Proc. 2005, 163 (7), 50.
(8) Chalmers, B; The plasticity of polycrystalline metals. In Plastic Deformation of Crystalline Solids. Mellon Institute, Pittsburgh, PA, May 19-20, 1950, pp. 193-198, with discussion.
(9) Clark, R.; Chalmers, B.: Mechanical deformation of aluminum bi-crystals. Acta Metall. 1954, 2, 80-86.
(10) Karashima, S; Studies on the plastic deformation of two-grained aluminum specimens.

Mem. Inst. Sci. Indust. Res., Osaka Univ., 1953, 10, 78-82.
(11) Pond, R.B.; Harrison, E.; Grain boundary movement in bi-crystalline aluminum. Trans. Amer. Soc. Met. 1958, 50, 994-1005, including discussion.
(12) Zaefferer, S.; Kuo, J.-C.; Zhao, Z.; Winning, M.; Raabe, D.; On the influence of the grain boundary misorientation on the plastic deformation of aluminum bi-crystals. Acta Mater. 2003, 51, 4719-4735.
(13) Aust, K.T.; Chalmers, B.; Structure of grain boundaries. In Deformation and Strength of Polycrystals; Armstrong, R.W.; Feltner, C.E., Eds.; Metall. Trans. 1970, 1, [5], 1095-1104.
(14) Armstrong, R.W.; Plasticity: Grain size effects. In Encyclopedia of Materials Science and Technology; Buschow, K.H.J.; Cahn, R.W.; Fleming, M.C.; et al., Eds.; Elsevier Science Ltd.: Oxford, 2001; 7103-7114.
(15) Smith, C.S.; Some elementary principles of polycrystalline microstructures. Metall. Rev. 1964, 9, 1-48.
(16) Rhines, F.N.; Craig, K.R.; DeHoff, R.T.; Mechanism of steady-state grain growth in aluminum. Metall. Trans. 1974, 5, 413-425.
(17) Hirsch, P.B.; A study of cold-worked aluminum by an x-ray micro-beam technique. III. The structure of cold-worked aluminum. Acta Cryst. 1952, 5, [2], 172-175.
(18) Hirsch, P.B.; Horne, R.W.; Whelan, M.J.; Direct observations of the arrangement and motion of dislocations in aluminum. Phil. Mag. 1956, 1, [7], 677-684. Reprinted in Special Issue: 50 Years of TEM of Dislocations, Phil. Mag. 2006, 86, [29-31], 4553-4572.
(19) Levy, I.J.; The structure of high-angle grain boundaries in aluminum. Phys. Stat. Sol. (b) 1969, 31, [1], 193-201.
(20) Le, G.M.; Godfrey, A.; Hansen, N.; Liu, W.; Winthur, G.; Huang, X.; Influence of grain size in the near-micrometer regime on the deformation microstructure in aluminum. Acta Mater. 2013, 61, 7072-7086.
(21) Armstrong, R.W.; Dislocation mechanics description of polycrystal plastic flow and fracturing behaviors. In Mechanics and Materials: Fundamentals and Linkages; Meyers, M.A.; Armstrong, R.W.; Kirchner, H.O.K., Eds.; John Wiley & Sons, Inc.: N.Y., 1999, Chap. 10, 363-398.
(22) Hong, C.; Huang, X.; Winthur, G.; Dislocation content of geometrically necessary boundaries aligned with slip planes in rolled aluminum, Phil. Mag. 2013, 93, [23], 3118-3141.
(23) Ball, C.J.; The flow stress of polycrystalline aluminum. Phil. Mag. 1957, 2, [20], 1011-1017.
(24) Weissmann, S.; Substructure characteristics of fine grained metals and alloys disclosed by x-ray reflection microscopy and diffraction analysis. Trans. Amer. Soc. Met. 52, 599- (1960).
(25) Hultgren, F.; Grain boundary and substructure hardening in aluminum. Trans. TMS-AIME 1964, 230, 898-903.
(26) Armstrong, R.W.; Bechtold, J.H; Begley, R.T.; Mechanisms of alloy strengthening in refractory metals. In Refractory Metals and Alloys II.; Semchyshen, M.; Perlmutter, I.; TMS-AIME Metallurgical Society Conferences; Interscience Publishers: N.Y., 1963, 17, 159-190.
(27) Hall, E.O.; The deformation and ageing of mild steel: Discussion of results. Proc. Phys. Soc. Lond. B 1951, 747-753.
(28) Petch, N.J.; The cleavage strength of polycrystals. J. Iron Steel Inst. 1953, 174, 25-28.
(29) Armstrong, R.W., Codd, I., Douthwaite, R.M. and Petch, N.J.; The plastic deformation of polycrystalline aggregates. Phil. Mag. 1962, 7, 45-58.

(30) Armstrong, R.W.; The yield and flow stress dependence on polycrystal grain size. In Yield, Flow and Fracture of Polycrystals; Baker, T.N., Ed.; Applied Science Publishers, Ltd.: London, 1983; 1-35.
(31) Carreker, R.P. Jr.; Hibbard, W.R. Jr.; Tensile deformation of aluminum as a function of temperature, strain rate and grain size. Trans. TMS-AIME 1957, 209, 1157-1163.
(32) Fleischer, R.L.; Hosford, W.F. Jr.; Easy glide and grain boundary effects in polycrystalline aluminum. Trans. TMS-AIME 1961, 221, 244-247.
(33) Hansen, N.; Effect of grain size and strain on the tensile flow stress of aluminum at room temperature. Acta Metall. 1977, 25, 863-869.
(34) Armstrong, R.W.; On size effects in polycrystal plasticity. J. Mech. Phys. Sol. 1961, 9, 196-199.
(35) Armstrong, R.W.; The influence of polycrystal grain size on mechanical properties. In Advances in Materials Research, Herman, H., Ed., John Wiley & Sons, Inc.: N.Y., 1970; 4, 101-146.
(36) Kim, K.-H.; Kim, H.-K.; Oh, S.-I.; Deformation behavior of pure aluminum specimen composed of a few grains during simple compression. J. Mater. Proc. Tech. 2006, 171, 205-213.
(37) Kwon, J.B.; Huh, H.; Kim, J.S.; Specimen and grain size effects on strain and strain rate hardening at various strain rates for Al1100. Exp. Mech. 2014, 54, 987-998.
(38) Keller, C.; Hug, E.; Hall-Petch behavior of Ni polycrystals with a few grains per thickness. Mater. Letts. 2008, 62, 1718-1720.
(39) Wyrzykowski, J.W.; Grabski, M.W.; The Hall-Petch relation in aluminum and its dependence on the grain boundary structure. Phil. Mag. 1986, 53, [4], 505-520.
(40) Armstrong, R.W.; Dislocation queueing analysis for the plastic deformation of aluminum polycrystals. In: Physics of Materials; A Festschrift for Dr. Walter Boas on the occasion of his 75th Birthday; Borland, D.W.; Clarebrough, L.M.; Moore, A.J.W., Eds.; University of Melbourne: Australia, 1979, 1-11.
(41) Fujita, H.; Tabata, T.; Effect of grain-size and deformation substructure on mechanical properties of polycrystalline aluminum. Acta Metall. 1973, 21, [4], 355-365.
(42) Hansen, N.; Flow stress and grain size dependence of non-ferrous metals and alloys. In The Yield, Flow and Fracture of Polycrystals; Baker, T.N., Ed.; Applied Science Publishers, Ltd.: London, 1983; 311-350.
(43) Hansen, N.; Ralph, B.; The strain and grain size dependence of the flow stress of copper. Acta Metall. 1982, 30, 411-417.
(44) Al-Haidary, J.T.; Petch, N.J.; de los Rios, E.R.; The plastic deformation of polycrystals. I. Aluminum between room temperature and 400°C. Phil. Mag. A 1983, 47, [6], 869-890.
(45) Al-Haidary, J.T.; Petch, N.J.; de los Rios, E.R.; The plastic deformation of polycrystals II. Aluminum at 77K. Phil. Mag. A 1983, 47, [6], 891-902.
(46) Al-Haidary, J.T.; Petch, N.J.; de los Rios, E.R.; The plastic deformation of polycrystalline aluminum. In The Yield, Flow and Fracture of Polycrystals; Baker, T.N., Ed.; Applied Science Publishers, Ltd.: London, 1983; 33-49.
(47) Maddin, R.: Mathewson, C.H.; Hibbard, W.R. Jr.; Unpredicted cross-slip in single crystals of alpha-brass. Trans TMS-AIME 1948, 175, 86-105; including discussion by Boas, W.; Ogilvie, G.J.
(48) Dorn, J.E.; Low temperature dislocation mechanisms. In Dislocation Dynamics; Rosenfield, A.R.; Hahn, G.T.; Bement, A.L. Jr.; Jaffee, R.I., Eds.; McGraw-Hill Book Co.: N.Y., 1968, 27-

55.
(49) Zerilli, F.J.; Armstrong, R.W.; Dislocation-mechanics-based constitutive equations for material dynamics calculations. J. Appl. Phys. 1987, 61, 1816-1825.
(50) Zerilli, F.J.; Armstrong, R.W.; Dislocation mechanics based constitutive equation incorporating dynamic recovery and applied to thermomechanical shear instability; In Shock Compression of Condensed Matter – 1997; Schmidt, S.C.; Dandekar, D.; Forbes, J.W., Eds.; Amer. Inst. Phys.: N.Y., 1998, 215-218.
(51) Zerilli, F.J.; Armstrong, R.W.; Constitutive relations for the plastic deformation of metals. In High-Pressure Science and Technology-1993; Schmidt, S.C.; Shaner, J.W.; Samara, G.A.; Ross, M., Eds.; Amer. Inst. Phys.: N.Y., Conf. Proc. 309, Part 2, 989-992.
(52) Paturi, U.M.R.; Narala, S.K.R.; Pundit, R.S.; Constitutive flow stress formulation, model validation and FE cutting simulation for AA7075-T6 aluminum alloy. Mater. Sci. Eng. A 2014, 605, 176-185.
(53) Baghani, M.; Eskandari, A.H.; Zakerzadeh, M.R.; Transient growth of a micro-void in an infinite medium under thermal load with modified Zerilli-Armstrong model. Acta Mech. 2016, 227, 943-953.
(54) Huang, H.; Asay, J.R.; Compressive strength measurements in aluminum for shock compression over the stress range of 4-22 GPa. J. Appl. Phys. 2005, 98, 033524.
(55) Huang, H.; Asay, J.R.; Reshock and release response of aluminum single crystal. J. Appl. Phys. 2007, 101, 063550.
(56) Vogler, T.J.; Ao, T.; Asay, J.R. High-pressure strength of aluminum under quasi-isentropic loading. Int. J. Plast. 2009, 25, 671-694.
(57) Armstrong, R.W.; Arnold, W.; Zerilli, F.J.; Dislocation mechanics of copper and iron in high rate deformation tests. J. Appl. Phys. 2009, 105, 023511.
(58) Moćko, W.; Rodriguez-Martinez, J.A.; Kowalewski, Z.L.; Rusinek, A.; Compressive viscoplastic response of 6082-T6 and 7075-T6 aluminum alloys under wide range of strain rate at room temperature: Experiments and modeling. Strain 2012, 48, 498-509.
(59) Swegle, J.W.; Grady, D.; Shock viscosity and the prediction of shock wave rise times. J. Appl. Phys. 1985, 58, 692-701.
(60) Crowhurst, J.C.; Armstrong, M.R.; Knight, K.B.; Zaug, J.M.; Behymer, E.M.; Invariance of the dissipative action at ultrahigh rates above the strong shock threshold. Phys. Rev. Lett. 2011, 107, 144302.
(61) Malygin, G.A.; Ogarkov, S.L.; Andriyash, A.V.; Dislocation structure of plastic relaxation waves in polycrystals and alloys under shock wave loading. (RU) Phys. Sol. State 2014, [11], 2239-2246.
(62) Gurrutxaga-Lerma, B.; Balint, D.S.; Dini, D.; Sutton, A.P.; The mechanisms governing the activation of dislocation sources in aluminum at different strain rates. J. Mech. Phys. Sol. 2015, 84, 273-292.
(63) Eshelby, J.D.; Frank, F.C.; Nabarro, F.R.N.; The equilibrium of linear arrays of dislocations. Phil. Mag. 1951, 7, 351-364.
(64) Zener, C.; A theoretical criterion for the initiation of slip bands, Phys. Rev. 1946, 69, 128-129.
(65) Zener, C.; The micro-mechanism of fracture. In Fracturing of Metals. Amer. Soc. Met.: Cleveland, OH, 1948, 3-31.
(66) Li, J.C.M.; Chou, Y.T.; The role of dislocations in the flow stress – grain size relationship. In

Strength and Deformation of Polycrystals. Fall meeting of TMS-AIME, Detroit, MI, October 14, 1968; Armstrong, R.W.; Feltner, C.E., Eds., Metall. Trans. 1970, 1, 1145-1158.
(67) Armstrong, R.W.; Dislocation pile-ups: From {110} cracking in MgO to model strength evaluations. Mater. Sci. Eng. A 2005, 409, 24-31.
(68) Armstrong, R.W.; Strength and strain rate sensitivity for nanopolycrystals, In Mechanical Properties of Nanocrystalline Materials, Li, J.C.M., Ed.; Pan Stanford Publishing Pte., Ltd.: Singapore, 2011, Ch. 3, 61-91.
(69) Petch, N.J.; Theory of the yield point and strain-ageing in steel, In Advances in Physical Metallurgy; Sir Alan Cottrell's 70th Birthday Meeting, Charles, J.A.; and Smith, G.C., Eds.; Inst. Met.: London, 1990; 11-25.
(70) Armstrong, R.W.; Material grain size and crack size influences on material fracturing. In Fracturing across the multi-scales of diverse materials. Armstrong, R.W.; Antolovich, S.D.; Griffiths, J.R.; Knott, J.F., Eds.; Phil. Trans. R. Soc. 2015, 373, [2038].
(71) Kang, J.-H.; Shanghong, D.; Kim, S.-J.; Bleck, W.; Grain boundary strengthening in high Mn austenitic steels. Metall. Mater. Trans A 2016, 47A, [5], 1918-1921.
(72) Bell, J.F.; Generalized large deformation behavior for face-centered cubic solid: Nickel, aluminum, gold, silver and lead. Phil. Mag. 1965, 11, 1135-1156.
(73) Pùschl, W.; Models for dislocation cross-slip in close-packed crystal structures: a critical review. Prog. Mater. Sci. 2002, 47, 415-461.
(74) Alankar, A.; Field, D.P.; Zbib, H.M.; Explicit incorporation of cross-slip in a dislocation density-based crystal plasticity model. Phil. Mag. 2012, 92, [24], 3084-3100.
(75) Armstrong, R.W.: Javadpour, S.; Dislocation mechanics description of plastic anisotropy and fracturing observations in textured Al-Li 2090-T8E41 alloy. In 4th International Conference on Aluminum Alloys; Their Physical and Mechanical Properties; Georgia Inst. Tech.: Atlanta, GA, 1994, II, 405-412.
(76) Thornton, P.R.; Mitchell, T.E.; Hirsch, P.B.; The dependence of cross-slip on stacking fault energy in face-centered cubic metals and alloys. Phil. Mag. 1962, [80], 1349-1369.
(77) Carreker, R.P., Jr.; Hibbard, W.P., Jr.; Tensile deformation of high-purity copper as a function of temperature, strain rate and grain size. Acta Metall. 1953, 1, [6], 654-663.
(78) Armstrong, R.W.; Strength and ductility of metals. Trans Indian Inst. Met. 1997, 50, [6], 521-531.
(79) Armstrong, R.W.; Theory for the tensile ductile-brittle behavior of polycrystalline h.c.p. materials; with application to beryllium. Acta Metall. 1968, 16, 347-355.
(80) Hughes, G.D., Smith, S.D.; Pande, C.S.; Johnson, H.R.; Armstrong, R.W.; Hall-Petch strengthening for the microhardness of 12 nanometer grain diameter electrodeposited nickel. Scr. Metall. 1986, 20, 93-97.
(81) Panin, V.E.; Armstrong, R.W.; Hall-Petch analysis for temperature and strain rate dependent deformation of polycrystalline lead. (RU) Phys. Mesomech. 2016, 19, [1], 1-6.
(82) Hansen, N.; Boundary strengthening in undeformed and deformed polycrystals. Mater. Sci. Eng. A 2005, 39-43.
(83) Dean, W.A., Zay Jeffries' contributions to aluminum metallurgy. ASM Met. Rev. 1966, 41, [5], 19-23, 41.
(84) Jeffries, Z.; Effect of temperature, deformation and grain size on the mechanical properties of metals. Trans. TMS-AIME 1919, 60, 474-576, with discussion.

(85) Hahn, T.A.; Armstrong, R.W.; Internal stress and solid solubility effects on the thermal expansivity of Al-Si eutectic alloys. Intern. J. Thermophys. 1988, 9, [2], 179-193.
(86) Hahn, T.A.; Armstrong, R.W.; Thermal expansion properties of 6061 Al alloy reinforced with SiC particles and short fibers. Intern. J. Thermophys. 1988, 9, [5], 861-871.
(87) Czerwinski, F.; Kasprzak, W.; Sediako, D.; Emadi, D.; Shaha, S.; Chen, D.; High-temperature aluminum alloys for automotive powertrains. Adv. Mater. & Proc. 2016, 174, [3], 16-20.
(88) Erginer, E.; Gurland, J.; Influence of composition and microstructure on strength of cast aluminum-silicon alloys. Zeitschr. f. Metallk. 1968, 61, [8], 606-.
(89) Liu, C.T.; Gurland, J. The strengthening mechanisms in spheroidized carbon steels. Trans. TMS-AIME 1968, 242, 1535-1542.
(90) Morrison, W.B.; Leslie, W.C.; The yield stress - grain size relation in iron substitutional alloys. Metall. Trans. 1973, 4, 379-381.
(91) Ansell, G.S.; Lenel, F.V.; Criteria for yielding of dispersion-strengthened alloys. Acta Metall. 1960, 8, [9], 612-616.
(92) Nakanishi, K.; Suzuki, H.; Analysis of the grain size dependence of the yield stress in copper-aluminum and copper nickel alloys. Trans. JPN Inst. Met. 1974, 15, 435ff.
(93) Suzuki, H.; Nakanishi, K.; A theory for the grain size dependence of the yield stress in face-centered cubic alloys. Trans. JPN Inst. Met. 1975, 16, [1], 17-27.
(94) Armstrong, R.W.; Douthwaite, R.M.; Hall-Petch basis for assessing alloy strengthening. In Grain Size and Mechanical Properties – Fundamentals and Applications. Otooni, M.A.; Armstrong, R.W.; Grant, N.J.; Ishizaki, K., Eds.; Mater. Res. Soc.: Pittsburgh, PA, 1995, 41-47.
(95) Tayon, W.; Crooks, R.; Domack, M.; Wagner, J.; Elmustafa, A.A.; EBSD study of delamination fracture in Al-Li alloy 2090. Exp. Mech. 2010, 50, 135-143.
(96) Antolovich, S.D.; Armstrong, R.W.; Plastic strain localization in metals. Prog. Mater. Sci. 2014, 59, 1-160.
(97) Portevin, A.; Le Chatelier, F.; Sur un phénomène observe lors de l'essai de traction d'alliages en cours de transformation . Comptes Rendus de l'Académe des Sciences 1923, 176, 507-510.
(98) McReynolds, A.W.; Plastic deformation waves in aluminum. Trans. TMS-AIME 1949, 185, 32-45.
(99) Cottrell, A.H.; A note on the Portevin-Le Chatelier Effect. Phil. Mag. 1953, 44, 829-832.
(100) Wagenhofer, M.; Ericson-Natishan, M.A.; Armstrong, R.W.; Zerilli, F.J.; Influences of strain rate and grain size on yield and serrated flow in commercial Al-Mg alloy 5086. Scr. Mater. 1999, 41, 1177-1184.
(101) Fernandez-Zelaia, P.; Adair, B.S.; Barker, V.M.; Antolovich, S.D.; The Portevin-Le Chatelier effect in Ni-based superalloy IN100. Metall. Mater. Trans. 2015, [12], 5596-5609.
(102) Armstrong, R.W.; Strength properties of ultrafine-grain metals. In Ultrafine-Grain Metals; Burke, J.J.; Weiss, V., Eds.; Syracuse University Press: Syracuse, N.Y., 1970, 1-35.
(103) Bonetti, E.; Pasquini, I.; Sampaolesi, E.; The influence of grain size on the mechanical properties of nanocrystalline aluminum. NanoStruct. Mater. 1997, 9, 611-614.
(104) Mukai, T.; Higashi, K.; Ductility enhancement of ultra fine-grained aluminum under dynamic loading. Scr. Mater. 2001, 44, 1493-1496.
(105) Hokka, M.; Kokkonen, J.; Seidt, J.; Matrka, T.; Gilat, A.; Kuokkala, V.-T.; High strain rate torsion properties of ultrafine-grained aluminum. Exp. Mech. 2012, 52, [2], 195-203.
(106) Khan, A.S.; Suh, Y.S.; Chen, X.; Takacs, L.; Zhang, H.; Nanocrystalline aluminum and iron:

Mechanical behavior at quasi-static and high strain rates and constitutive modeling. Int. J. Plast. 2006, 22, 195-209.
(107) Huang, X.; Kamikawa, N.; Hansen, N.; Strengthening mechanisms in nanostructured aluminum. Mater. Sci. Eng. A 2008, 483-484, 102-104.
(108) Bazarnik, P.; Huang, Y.; Lewandowska, M.; Langdon, T.G.; Structural impact on the Hall-Petch relationship in an Al-5Mg alloy processed by high-pressure torsion. Mater. Sci. Eng. A 2015, 626, 9-15
(109) Meyers, M.A.; Mishra, A.; Benson, D.J.; Mechanical properties of nanocrystalline materials. Prog. Mater. Sci. 2006, 51, 427-556.
(110) Li, J.C.M., Ed.; Mechanical Properties of Nanocrystalline Materials. Pan Stanford Publishing Pte. Ltd.: Singapore, 2011, 1-332.
(111) Armstrong, R.W.; Hall-Petch analysis for nanopolycrystals. In Nanometals – Status and Perspective; 33rd Risö International Symposium on Materials Science. Faester, S.; Hansen, N.; Huang, X.; Juul Jensen, D.; Ralph, B., Eds.; Technical University of Denmark: Roskilde Campus, DK, 2012, 181-199.
(112) Narutani, T.; Takamura, J.; Grain size strengthening in terms of dislocation density measured by resistivity. Acta Metall. 1991, 39, [8], 2037-2049.
(113) Tsuji, N.; Ito, Y.; Saito, Y.; Minamino, Y.; Strength and ductility of ultrafine grained aluminum and iron produced by ARB and annealing. Scr. Mater. 2002, 47, [12], 893-899.
(114) Lu, L.; Chen, X.; Huang, X.; Lu, K.; Revealing the maximum strength in nanotwinned copper. Science 2009, 323, 607-610.
(115) Torrents, A.; Yang, H.; Mohammed, F.; Effect of annealing on hardness and the modulus of elasticity in bulk nanocrystalline nickel. Metall. Mater. Trans. A. 2010, 41A, 621-630.
(116) Hu, T.; Jiang, L.; Yang, H.; Ma, K.; Topping, T.D.; Yee, J.; Li, M.; Mukherjee, A.K.; Schoenung, J.M.; Lavernia, E.J.; Stabilized plasticity in ultrahigh strength, submicron Al crystals. Acta Mater. 2015, 94, 46-58.
(117) Armstrong, R.W.; In Defect Structures in Solids; Vasu, K.I.; Raman, K.; Sastry, D.H.; Prasad, Y.V.R.K., Eds.; Indian Institute of Science: Bangalore, IN, 1972, 306-313; see J. Sci. Indust. Res. 1973, 32, 591-598.
(118) Prasad, Y.V.R.K.; Armstrong, R.W.; Polycrystal versus single-crystal strain rate sensitivity of cadmium. Phil. Mag. 1974, 29, 1421-1425.
(119) Armstrong, R.W.; Li, Q.Z.; Dislocation mechanics of high-rate deformations. Metall. Mater. Trans. A 2015, 46A, 4438-4453.
(120) Armstrong, R.W.; Rodriguez, P.; Flow stress/grain size/strain rate coupling for fcc nanopolycrystals. Phil. Mag. 2006, 86, 5787-5796.
(121) Asaro; R.J.; Suresh, S.; Mechanistic models for the activation volume and rate sensitivity in metals with nanocrystalline grain sizes. Acta Mater. 2005, 53, 3369-3382.
(122) Weng, G.J.; A composite model of nanocrystalline materials. In Mechanical Properties of Nanocrystalline Materials; Li, J.C.M., Ed.; Pan Stanford Publishing Pte., Ltd.: Singapore, 2011, Chap. 4, 93-131.
(123) May, J.; Höppel, H.W.; Göken, M.; Strain rate sensitivity of ultrafine-grained aluminum processed by severe plastic deformation. Scr. Mater. 2005, 53, 189-194.
(124) Armstrong, R.W.; Grain size strengthening and weakening in polycrystals. Canad. Metall. Quart. 1974, 13, 187-202.

(125) Balsubramanian, N.; Langdon, T.G.; An analysis of superplastic flow after processing by ECAP. Mater. Sci. Eng. A 2005, 410, 476-479.
(126) Balasubramanian, N.; Langdon, T.G.; The strength-grain size relationship in ultrafine-grained metals. Metall. Mater. Trans. A, published online 11 April 2016.
(127) Pande, C.S.; Cooper, K.P.; Nanomechanics of Hall-Petch relationship in nanocrystalline materials. Prog. Mater. Sci. 2009, 54, 689-706.
(128) Mompiou, F.; Legros, M.; Boé, A.; Coulombier, M.; Raskin, J.-P.; Pardoen, T.; Inter- and intragranular plasticity mechanisms in ultrafine-grained Al thin films: An in-situ TEM study. Acta Mater. 2013, 61, 213-216.
(129) Padmanabhan, K.A.; Sripathi, S.; Hahn, H.; Gleiter, H.; Inverse Hall-Petch effect in quasi- and nanocrystalline materials. Mater. Letts. 2014, 133, 151-154.
(130) Kong, Q.P.; Fang, Q.F.; Progress in the investigation of grain boundary relaxation. Crit. Rev. Sol. State & Mater. Sci. 2016, 41, [3], 192-216.
(131) Petch, N.J.; Armstrong, R.W.; The tensile test. Acta Metall. Mater. 1990, 38, 2695-2700.
(132) Armstrong, R.W.; Zerilli, F.J.; Dislocation mechanics aspects of plastic instability and shear banding. In Shear Instabilities and Viscoplasticity Theories; Armstrong, R.W.; Batra, R.C.; Meyers, M.A.; Wright, T.W., Eds.; Mech. Mater. 1994, 17, 319-327.
(133) Kamikawa, N.; Huang, X.; Tsuji, N.; Hansen, N.; Strengthening mechanisms in nanostructured high-purity aluminum deformed to high strain and annealed. Acta Mater. 2009, 57, 4198-4208.
(134) Basinski, Z.S.; The instability of plastic flow of metals at very low temperatures. Proc. R. Soc. Lond. 1957, A240, 229-242.
(135) Chin, G.Y.; Hosford, W.F.; Backofen, W.A.; Ductile fracture of aluminum. Trans. TMS-AIME 1964, 230, 437-449.
(136) Armstrong, R.W.; Strengthening mechanisms and brittleness in metals. J. Ocean. Eng. 1969, 1, 239-256.
(137) Lassance, D.; Fabrègue, D.; Delannay, F.; Pardoen, T.; Micromechanics of room and high temperature fracture in 6xxx Al alloys. Prog. Mater. Sci. 2007, 52, 62-129.
(138) Khadyko, M.; Myhr, O.R.; Dumoulin, S.; Hopperstad, O.S.; A microstructure-based yield stress and work-hardening model for textured 6xxx aluminum alloys. Phil. Mag., 2016, 96, [11], 1047-1072.
(139) Shakoorie Oskooie, M.; Asgharzadeh, H.; Kim, H.S.; Microstructure, plastic deformation and strengthening mechanisms of an Al-Mg-Si alloy with a bimodal grain structure. J. Alloys Comp. 2015, 632, 540-548.
(140) Antolovich, S.D.; Armstrong, R.W.; A dislocation pile-up computation for adiabatic shear banding. In Materials Fundamentals of Fatigue and Fracture. Mater. Res. Soc.: Warrendale, PA, 2014, Proc. Vol. 1650.
(141) Armstrong, R.W.; Coffey, C.S.; Elban, W.L.; Adiabatic heating at a dislocation pile-up avalanche. Acta Metall. 1982, 30, 2111-2118
(142) Armstrong, R.W.; Elban, W.L.; Temperature rise at a dislocation pile-up breakthrough. Mater. Sci. Eng. 1989, A122, L1-L3.
(143) Owolabi, G.M.; Bolling, D.T.; Tiamiyu, A.A.; Abu, R.; Odeshi, A.G.; Whitworth, H.A.; Shear strain localization in AA 2219-T8 alloy at high strain rates. Mater. Sci. Eng. A 2016, 655, 212-220.
(144) Forsyth, P.J.E.; Stubbington, C.A.S.; A slip-band extrusion effect observed in pure aluminum.

Nature 1955, 175, [4461], 767-768.
(145) Forsyth, P.J.E.; Discussion Meeting: Slip-band damage and extrusion. Proc. Roy. Soc. Lond. A 1957, 242, [1229], 198-202.
(146) Cottrell, A.H.; Hull. D.; Extrusion and intrusion by cyclic slip in copper. Proc. R. Soc. Lond. A 1957, 242, 211-213.
(147) Thompson, N.; Wadsworth, N.J.; Louat, N.; The origin of fatigue fracture in copper. Phil. Mag. 1956, 1, 113-126.
(148) Armstrong, R.W.; Sir Alan Cottrell and the dislocation mechanics of fracturing. Int. J. Str., Fract. Complex. 2013/2014, 8, 105-115.
(149) Broom, T.; Whittaker, V.N.; Slip during fatigue of an age-hardened alloy. Nature 1956, 486-487 (1956).
(150) Broom, T.; Cross-slip as a significant mechanism in the fatigue of metals. Acta Cryst. 1960, 13, [12], 1123.
(151) Armstrong, R.W.; Phillips, W.L.; The influence of specimen size, polycrystal grain size and yield point behavior on the fatigue strength of low-carbon steel. J. Mech. Phys. Sol. 1969, 17, 265-270.
(152) Turnbull, A.; De Los Rios, E.R.; The effect of grain size on the fatigue of commercially pure aluminum. Fatigue, Fract. Engng Mater. Struct. 1995, 18, [12], 1455-1467.
(153) El-Madhoun, Y.; Mohamed, A.; Bassim, M.N. ; Cyclic stress-strain response and dislocation structures in polycrystalline aluminum. Mater. Eng. A 2003, 339, 220-227.
(154) Baxter, W.J.; Wang, P.C.; Finite element predictor of high cycle fatigue life of aluminum alloys. Metall. Trans. A. 1990, 21A, 1151-1159.
(155) Zhang, Z.F.; Wang, Z.G.; Grain boundary effects on cyclic deformation and fatigue damage. Prog. Mater. Sci. 2008, 53, 1025-1099.
(156) Höppel, H.W.; Kautz, M.; Murashkin, M.; Langdon, T.G.; Valiev, R.Z.; Mughrabi, H. An overview: Fatigue behavior of ultrafine grained metals and alloys. Int. J. Fatigue 2006, 28, 1001-1010.
(157) Lukáš, P.; Kunz, L.; Navratalova, L.; Bokuvka, O.; Fatigue damage of ultrafine-grain copper in very-high cycle fatigue region. Mater. Sci. Eng. A 2011, 528, 7036-7040.
(158) Armstrong, R.W.; 60 years of Hall-Petch: Past to present nano-scale connections. (JPN) Mater. Trans. 2014, 55, [1], 2-12.
(159) Valiev, R.Z.; Estrin, Y.; Horita, Z.; Langdon, T.G.; Zehetbauer, M.J.; Zhu, Y.T.; Producing bulk ultrafine-grained materials by severe plastic deformation: Ten years later. JOM 2016, 68, [4], 1216-1226.

---

*Invited for **Encyclopedia of Aluminum and Its Alloys**; G.E. Totton and M. Tiryakioglu, editors; Taylor & Francis Group, Publishers, U.K., submitted March 20, 2016.